Naturally secreted oligomers of amyloid β protein potently inhibit hippocampal long-term potentiation *in vivo*

Dominic M. Walsh*, Igor Klyubin†, Julia V. Fadeeva*, William K. Cullen†, Roger Anwyl‡, Michael S. Wolfe*, Michael J. Rowan† & Dennis J. Selkoe*

** Department of Neurology, Harvard Medical School and Center for Neurologic Diseases, Brigham and Women's Hospital, Boston, Massachusetts 02115, USA*
† Departments of Pharmacology and Therapeutics and ‡ Physiology, Trinity College, Dublin 2, Ireland

Although extensive data support a central pathogenic role for amyloid β protein (Aβ) in Alzheimer's disease[1], the amyloid hypothesis remains controversial, in part because a specific neurotoxic species of Aβ and the nature of its effects on synaptic function have not been defined *in vivo*. Here we report that natural oligomers of human Aβ are formed soon after generation of the peptide within specific intracellular vesicles and are subsequently secreted from the cell. Cerebral microinjection of cell medium containing these oligomers and abundant Aβ monomers but no amyloid fibrils markedly inhibited hippocampal long-term potentiation (LTP) in rats *in vivo*. Immunodepletion from the medium of all Aβ species completely abrogated this effect. Pretreatment of the medium with insulin-degrading enzyme, which degrades Aβ monomers but not oligomers, did not prevent the inhibition of LTP. Therefore, Aβ oligomers, in the absence of monomers and amyloid fibrils, disrupted synaptic plasticity *in vivo* at concentrations found in human brain and cerebrospinal fluid. Finally, treatment of cells with γ-secretase inhibitors prevented oligomer formation at doses that allowed appreciable monomer production, and such medium no longer disrupted LTP, indicating that synaptotoxic Aβ oligomers can be targeted therapeutically.

Fibrillar (but not monomeric) forms of Aβ akin to those present in the amyloid plaques of Alzheimer's disease are neurotoxic in culture[2,3]. However, relatively weak correlations between fibrillar plaque density and severity of dementia are found in Alzheimer's diseased brains[4,5], whereas correlations between soluble Aβ levels and the extent of synaptic loss and cognitive impairment are stronger[6,7]. SDS-stable Aβ oligomers (of relative molecular masses M_r ~8,000 and ~12,000) have been detected by western blotting in the buffer-soluble fraction of Alzheimer's diseased cortex[7]. These are strikingly similar to soluble, SDS-stable Aβ oligomers produced by certain cultured cells[8–10]. We previously confirmed the latter species as Aβ oligomers by amino-terminal radiosequencing and precipitation with carboxy-terminal-specific antibodies[8,10]. The levels of these oligomers are specifically augmented by expressing Alzheimer's disease-causing mutations in amyloid precursor protein (APP) or presenilin that increase Aβ42 production[11], supporting their pathological relevance. Importantly, young APP transgenic mice undergo synaptic, electrophysiological and behavioural changes before any amyloid plaque formation[12,13], but the nature of the responsible Aβ species in the brain cannot be specifically defined.

To assess the subcellular origin of naturally occurring Aβ oligomers secreted by cells expressing human APP, we prepared microsomes from 7PA2 Chinese hamster ovary (CHO) cells, which stably express the V717F Alzheimer's disease mutation in APP_{751} (an APP:isoform 751 amino acids in length)[8,10]. A highly sensitive immunoprecipitation/western blot method[10] revealed both monomers and oligomers of Aβ in the isolated, washed microsomes, and the Aβ dimers in the microsomes co-migrated with those in the conditioned medium (CM) (Fig. 1a). Previous trypsinization of the intact cells did not alter the amounts of the various Aβ assemblies recovered in the microsomes (Fig. 1a, lanes 7 versus 8), supporting their intracellular origin. The co-migrating dimers and trimers present in CM reacted with antibodies specific to the C termini of Aβ40 and Aβ42 (Fig. 1a, lanes 3 and 4). The oligomeric bands were not altered by pre-treatment with 8 M urea or 50% formic acid (Fig. 1b). Previously, radiosequencing of these monomer, dimer and trimer bands in 7PA2 CM confirmed that they are composed of Aβ[8].

Extensive immunoelectron microscopy, which readily detects synthetic Aβ protofibrils in the CM of cultured cells[14], revealed no such filamentous assemblies in 7PA2 CM (not shown). Ultracentrifugation of the CM at a force (100,000*g* × 3 h) that sediments synthetic Aβ fibrils and protofibrils did not bring down any Aβ

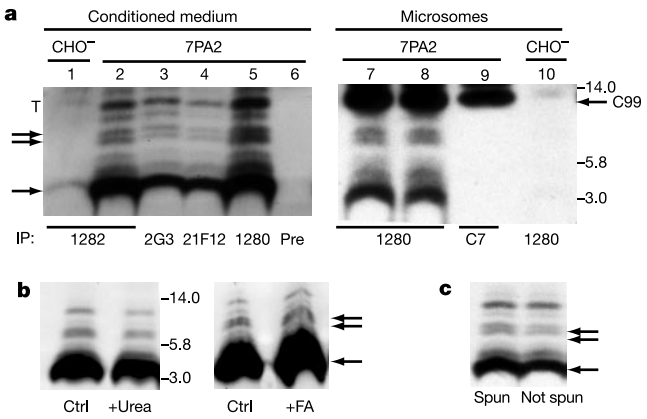

Figure 1 SDS-stable oligomers of Aβ are produced intracellularly and secreted. **a**, 7PA2 (lanes 2–6) and CHO^- (lane 1) conditioned medium (CM) were immunoprecipitated (IP) with antibodies or preimmune serum (Pre) and western blotted with monoclonal antibody 6E10. Microsomes from either 7PA2 (lanes 7–9) or CHO^- (land 10) cells were incubated with (lane 7) or without (lanes 8, 10) trypsin, lysed and precleared with APP C-terminal antiserum, C7 (pellet shown, lane 9). Precleared, lysates were then precipitated with R1280 (lanes 7, 8 and 10). The Aβ trimer in microsomal lysates is obscured by residual APP C-terminal fragment, C99 (compare lanes 7–9 with lanes 2–5). Arrow, monomeric Aβ; double arrow, dimeric Aβ; T, trimer. **b**, Incubation of the R1282 precipitate of 7PA2 CM in either 8 M urea or 50% formic acid did not alter oligomers. **c**, Centrifugation of CM at 100,000*g* × 3 h did not alter oligomer amounts. Relative molecular masses (M_r × 1,000) are shown on the right-hand side of gel lanes in **a**, **b**, Figs 2, 3c–e and 4d, h.

assemblies, and the amount of oligomers in the supernatant was unaltered (Fig. 1c).

Next, we fractionated total 7PA2 microsomes on discontinuous iodixanol gradients[15] and compared the distribution of the oligomers with those of organelle marker proteins. Aβ immunoreactive bands at M_r 4K, 6K and 8K–9K were principally present in fractions 4–7, which were enriched in Golgi-type vesicles (syntaxin-6-positive) and recycling endosomes (transferrin-receptor-positive) but contained only low levels of endoplasmic reticulum proteins (Grp 78 and calnexin) (Fig. 2 and not shown). The microsomal Aβ species co-migrated with the previously confirmed oligomers in the CM (Fig. 2d) and were unreactive with an APP C-terminal antibody (C7) (Fig. 2d) or preimmune serum (not shown). Immunoprecipitation of the subcellular vesicles with antibodies to the free C termini of Aβ40 (2G3) and Aβ42 (21F12) revealed a faint Aβ species of M_r 12K, a putative trimer, in addition to monomers and dimers (not shown). These were again principally localized to iodixanol gradient fractions 4–7, in which Aβ has previously been shown to be generated[15]. These data suggest that Aβ oligomerization is initiated soon after the generation of Aβ in discrete intracellular vesicles.

To determine whether these cell-derived oligomers of human Aβ have biological activity *in vivo*, we examined the effect of 7PA2 CM on hippocampal LTP, a measure of synaptic plasticity that is exquisitely sensitive to disruption by synthetic Aβ[16]. Long-term potentiation of excitatory synaptic transmission in the CA1 area of anaesthetized rats was induced by high-frequency stimulation (HFS). Microinjection of 7PA2 CM (1.5 μl intracerebroventricular, i.c.v.) completely blocked LTP at 3 h post-stimulation; only a waning potentiation lasting <90 min was elicited (Fig. 3a, g). In contrast, a robust LTP that was stable for over 3 h was induced after identical infusion of CM (1.5 μl) from untransfected CHO^- sister cultures (Fig. 3a, g). The LTP block was not related to any decrease in baseline transmission, because 7PA2 CM did not alter synaptic responses (EPSPs) in the absence of HFS (Fig. 3a, g).

The CM of CHO^- and 7PA2 cells should be indistinguishable except for the presence in the latter of the secretory products of human APP metabolism: APP_S, Aβ and p3 (Aβ17–40/42). To determine if Aβ caused the LTP block, we compared the effects of

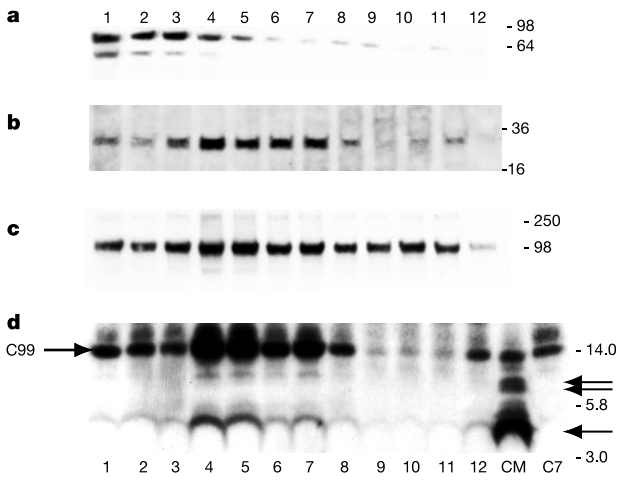

Figure 2 SDS-stable oligomers are formed soon after generation of Aβ. Microsomes fractionated on discontinuous iodixanol gradients[15] were lysed and blotted for Grp78 (**a**), syntaxin 6 (**b**) and transferring receptor (**c**). The remainder of each fraction was precleared with C7-protein A (as in Fig. 1) and then precipitated with R1280, and Aβ species blotted with 6E10 (**d**). CM, medium from the same cells. C7, aliquot of fraction 4, precipitated with C7. Arrow, monomeric Aβ; double arrow, dimeric Aβ. Data are typical of four fractionations.

7PA2 CM before and after immunodepletion with R1282, a high-titre polyclonal Aβ antibody. R1282 immunodepletion completely prevented the block of LTP (Fig. 3b, g). Western blotting confirmed that R1282 efficiently precipitated both Aβ monomers and oligomers; a second immunoprecipitation brought down very little additional protein (Fig. 3c). By enzyme-linked immunosorbent assay (ELISA), the R1282 precipitation decreased total Aβ in CM from 5,475 ± 897 to $1,253 \pm 24\ \mathrm{pg\,ml^{-1}}$ (mean ± s.d., $n = 3$). APP_S was poorly precipitated by R1282 (not shown). Correspondingly, the amounts of APP_S remaining in CM before and after R1282 immunoprecipitation were indistinguishable (Fig. 3d). The abrogation of the LTP block by R1282 was not due to a nonspecific effect of the immunodepletion or to an undetected decrease in APP_S concentration, because immunodepletion of 7PA2 CM with a polyclonal antibody (B5) to APP_S had no effect (Fig. 3b, g). The addition of R1282 to CHO^- CM likewise did not affect LTP induction (Fig. 3g).

Because neither the Aβ ELISA nor the immunoprecipitation/western blot assay recognizes p3 (ref. 10), we addressed the possibility that p3 in the 7PA2 CM mediated the observed block of LTP. Synthetic human p3 added to CHO^- CM at a concentration (11.5 nM) well in excess of that found in 7PA2CM[8] did not affect LTP (Fig. 3h).

Next, we asked whether the block of LTP was due to the abundant Aβ monomers or to the less abundant but invariably present SDS-stable Aβ oligomers. To do so, we took advantage of the specificity of insulin-degrading enzyme (IDE) to selectively degrade and remove Aβ monomers from CM (Fig. 3e)[17]. 7PA2 CM was divided into three equal aliquots: one was held at 4 °C, another was incubated at 37 °C for 12 h, and the third was incubated with purified IDE at 37 °C for 12 h. The latter incubation caused complete loss of detectable Aβ monomer, while leaving the Aβ oligomers virtually unchanged (Fig. 3e, lane 2). The CM aliquot incubated without IDE underwent only a slight decrease in Aβ monomer (Fig. 3e, lane 3). Both the second and third aliquots still caused a block of LTP at 3 h (Fig. 3f, h) that was indistinguishable from that of the first (untreated) aliquot. That IDE itself blocked LTP was excluded when (1) injection of plain medium spiked with IDE did not alter LTP (Fig. 3h), and (2) infusion of IDE-treated 7PA2 CM from which the His-tagged IDE had been removed by metal affinity chromatography still blocked LTP (Fig. 3h, IDE plus MAC). We conclude that naturally secreted, soluble human Aβ oligomers are specifically responsible for the block of hippocampal LTP by 7PA2 CM.

Because LTP was selectively blocked by Aβ oligomers in the absence of monomers, protofibrils or fibrils, we pharmacologically prevented oligomer formation in living cells while retaining substantial monomer production and assessed whether this would preserve normal LTP. We synthesized two structurally dissimilar γ-secretase inhibitors that dose-dependently inhibited Aβ secretion by 7PA2 cells: DAPM (half-maximal inhibitory concentration, IC_{50} ~10 nM) and MWIII-20 (IC_{50} ~10 μM)) (Fig. 4a, b). After treatment of cells for 6 h with 10 μM MWIII-20, the dimer (M_r 8K) was only faintly detectable by immunoprecipitation/western blot, whereas ~60% of the monomer signal remained (Fig. 4c, e). For MWIII-20, the IC_{50} for monomers by this method was ~30 μM, whereas that for dimers was ~10-fold lower. With the more potent DAPM, the IC_{50} for monomers was ~0.1 μM, whereas that for dimers was ~20-fold lower. Thus, at 0.1 μM, DAPM decreased monomers, but there was a relatively greater loss of dimers, which were now barely or not detectable (Fig. 4d). The percentage decrease of dimer at each concentration was greater than that of monomer in all experiments, and these two values were significantly different at the higher concentrations ($P < 0.005$) (Fig. 4e, f, asterisks). On the basis of these results, we treated 7PA2 cells for 6 h with 0.1 μM DAPM, confirmed the marked decrease in oligomer levels in this CM (Fig. 4h) and then microinjected an aliquot (1.5 μl i.c.v.) into rats. High-frequency stimulation produced a robust LTP which was

fully maintained for over 180 min (Fig. 4g, red symbols). This LTP was indistinguishable from that observed after injection of CHO^- CM spiked with the same or greater concentrations of DAPM (1 μM, 144 ± 8%, $n = 3$). To control further for the presence of the inhibitor and the fact that treatment with DAPM reduced Aβ monomer production by ~40%, 7PA2 CM was diluted 1:1 with plain DMEM, and DAPM spiked in (to 0.1 μM) just before injection. In contrast to the results obtained using CM from DAPM-treated cells, injection of this diluted 7PA2 CM spiked with DAPM caused a block of LTP typical of that observed previously ($P < 0.05$, Fig. 4g, blue symbols).

These experiments allow us to attribute an inhibition of hippocampal LTP *in vivo* specifically to oligomers, not monomers or fibrils, of naturally secreted human Aβ. The ability to collect heterogeneous human Aβ species produced naturally by living cells, combined with the property of IDE to degrade Aβ monomers but not oligomers, enabled us to specify that SDS-stable oligomers of Aβ consistently block hippocampal LTP. In addition to the advantages of this approach over treatments using synthetic Aβ, it provides specificity about the form of Aβ responsible for biological activity that is not achievable in APP transgenic mouse brains. The work demonstrates for the first time that a biochemically defined oligomeric assembly of naturally secreted human Aβ alters hippocampal synaptic efficacy at physiological levels. Our findings strongly support the emerging hypothesis that soluble Aβ oligomers are the principal effectors of the synaptic dysfunction and loss that characterize Alzheimer's disease[7,12–14,18–20]. Importantly, the CM we microinjected contained total human Aβ concentrations (mean ± s.d. : 3,223 ± 1,217 pg ml^{-1}; $n = 9$) very similar to those we previously measured in normal human cerebrospinal fluid (4,003 ± 1,873 pg ml^{-1}, $n = 32$)[10].

We provide evidence that after their genesis in intracellular vesicles, Aβ monomers form dimers, trimers and perhaps higher oligomers (Figs 1 and 2), that at least a portion of these oligomers is highly stable, and that some are subsequently secreted (Fig. 1b). The secreted oligomers can interact with neurons *in vivo*, altering their normal physiology (Fig. 3). Analogous effects may underlie the subtle synaptic changes and impairment of learning and memory documented in young APP transgenic mice[12,13,20–21] and in early Alzheimer's disease patients themselves. Our findings do not rule out an additional role for subsequent morphological lesions that characterize Alzheimer's disease and certain transgenic mouse models[22].

Synthetic Aβ oligomers block rat hippocampal LTP[18] but involve substantially higher doses of single synthetic Aβ species. In transgenic mice overexpressing human APP, some studies report failure

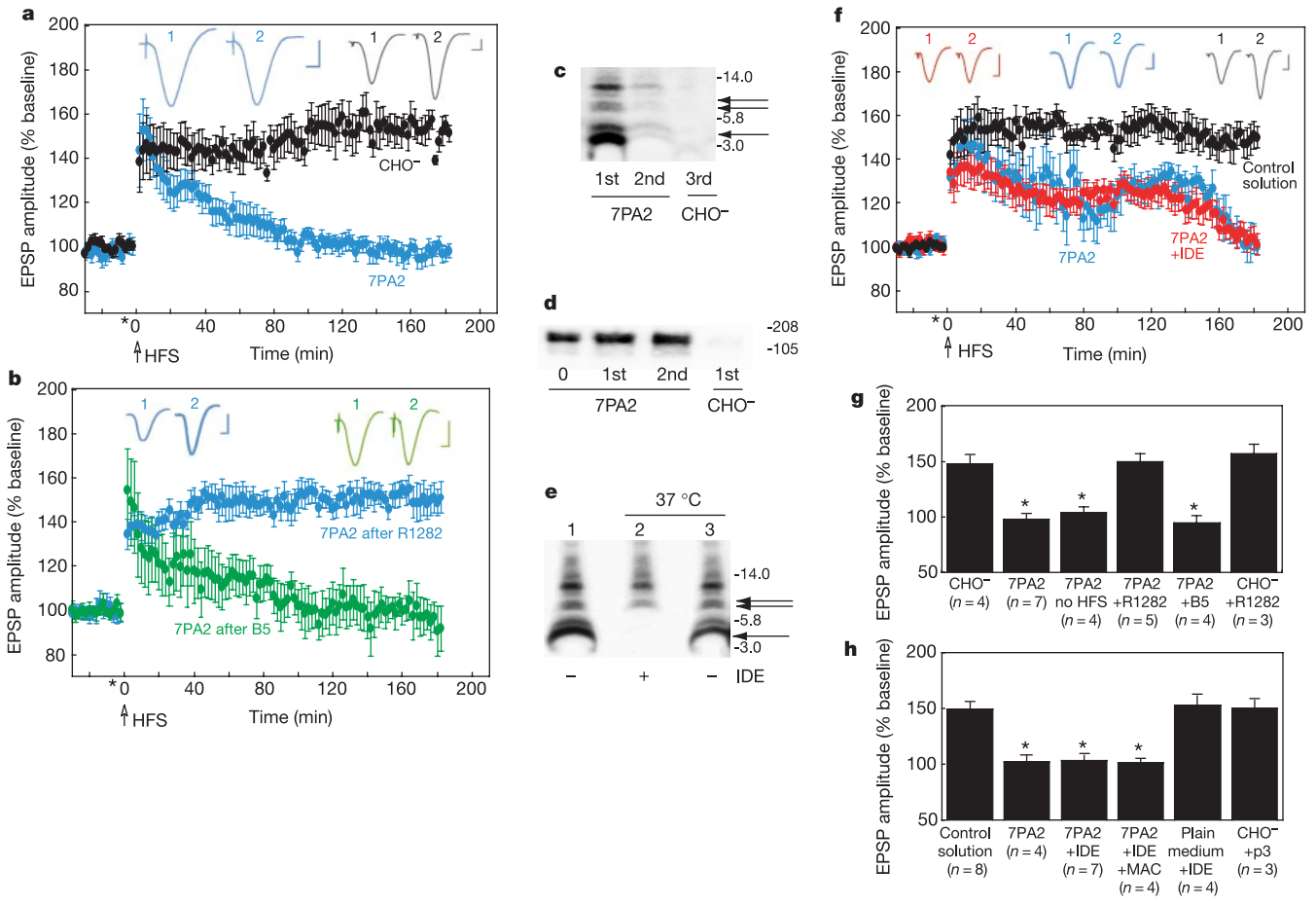

Figure 3 SDS-stable oligomers of human Aβ block hippocampal LTP *in vivo*. **a**, 7PA2 CM (blue) but not CHO^- CM (black, $P < 0.001$) blocked LTP. Insets show typical EPSPs ~5 min pre- (1) and ~3 h post-HFS (2); calibration bars 5 ms/0.5 mV. **b**, Immunoprecipitation of 7PA2 CM with an antibody to Aβ (R1282, blue, see **c**) but not to APP_S (B5, green) prevented the block of LTP. **c**, Blots of R1282 precipitates from CM used in **b** show that Aβ monomer (arrow) and dimer (double arrow) had been efficiently precipitated; compare Aβ retrieved in 1st precipitate versus in a second precipitation (2nd). **d**, Blotting of remaining CM of samples in **c** with 22C11 revealed that the R1282 precipitation did not alter APP_S-α levels. **e**, Incubation of 7PA2 CM with IDE caused complete loss of Aβ monomers (single arrow), whereas Aβ dimers (double arrow) and trimers were minimally diminished (lanes 1 versus 2). **f**, Treatment of 7PA2 CM with IDE (red) did not prevent the block of LTP. **g**, **h**, Magnitudes of LTP at 3 h post-HFS (% baseline ± s.e.m.); asterisks $P < 0.05$ compared to CHO^- (**g**) or control solution (**h**). *n*, Number of animals used per treatment.

of LTP maintenance in 4–5 month old[23], 5–7 month old[24] or 16 month old[25] animals, whereas others find impaired synaptic transmission but no change in LTP at 8–10 months[12] or 12–18 months[26]. Such studies of transgenic mice lack an advantage of our paradigm, namely the ability to study the effects of biochemically defined assembly forms of naturally produced human Aβ at physiological levels, in the absence of any confounding effects of APP overexpression.

An attractive therapeutic approach to Alzheimer's disease would be to reduce selectively the levels of potentially synaptotoxic Aβ oligomers. We show that two chemically distinct, cell-penetrant γ-secretase inhibitors block Aβ dimer and trimer formation at doses which allow appreciable monomer production. In contrast, anti-aggregation compounds would need to be both cell-penetrant and capable of blocking very early Aβ oligomerization; if such molecules did not prevent initial dimerization, they might enhance the levels of potentially synaptotoxic species. Thus, Aβ-lowering compounds (for example, β- or γ-secretase inhibitors) that prevent intra- and extracellular oligomerization while still allowing significant monomer production would be particularly desirable. Because stable oligomers can potentially arise from a large variety of proteins, both those already implicated in disease[27] and those that are not[28], the prevention of oligomer formation by reducing monomer concentrations could have wide relevance to the treatment of protein-folding disorders. □

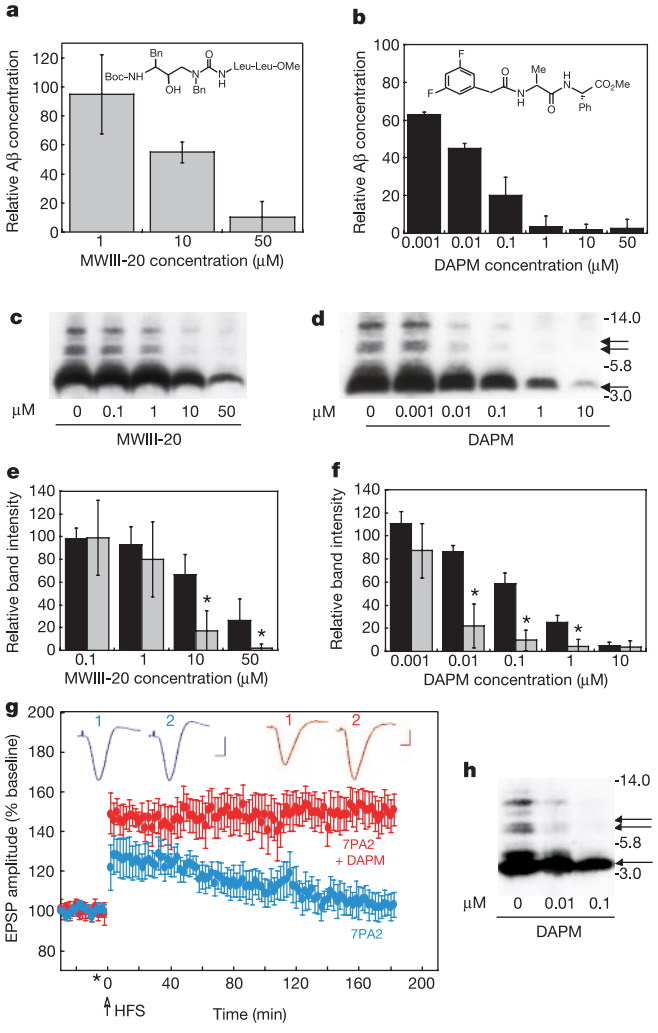

Figure 4 γ-secretase inhibitors block Aβ oligomer formation at doses that allow substantial monomer production. Inhibition of 7PA2 cellular Aβ secretion by MWIII-20 (**a**) and DAPM (**b**) was quantified by ELISA. Values (means ± s.d.) from three independent experiments were normalized to DMSO controls. Insets show inhibitor structures. **c**, **d**, 7PA2 cells were treated for 6 h with MWIII-20 or DAPM and Aβ species visualized by immunoprecipitation and western blot. **e**, **f**, Densitometric quantification of experiments as in **c** and **d**; Aβ monomer (black bars) and dimer (grey bars) densities normalized to vehicle control. MWIII-20, $n = 8$ and DAPM, $n = 5$. Asterisk indicates that at a given concentration, decrease in dimer is significantly greater ($P < 0.005$) than decrease in monomer. **g**, CM from cells treated with 0.1 μM DAPM (red, $n = 5$) allowed a robust LTP, whereas media from untreated 7PA2 cells (blue, $n = 4$) blocked LTP (insets as in Fig. 3). **h**, 7PA2 cells were conditioned in plain DMEM with or without DAPM for 6 h; CM was examined by immunoprecipitation and western blot and used for electrophysiology.

Methods

APP-expressing cells

Chinese hamster ovary cells stably transfected with a complementary DNA coding for APP751 containing the Val717Phe familial Alzheimer's disease mutation (referred to as 7PA2 cells) were cultured in Dulbecco's modified Eagle's medium (DMEM) with 10% fetal bovine serum as described[8,10].

Immunoprecipitation/western blot analysis

Aβ monomers and oligomers were visualized using a highly sensitive immunoprecipitation/western blot protocol that can readily detect as little as 200 pg of naturally secreted human Aβ[10]. For quantification of band intensity, appropriate film exposures were scanned and the density of bands determined with AlphaEase software (AlphaInnotech).

Subcellular fractionation

Total cellular microsomes were prepared from thirty 10-cm dishes of 7PA2 cells (~3×10^8 cells), and fractionated on iodixanol step gradients essentially as described previously[15]. The resulting gradient was fractionated into 1-ml aliquots and a 100 × stock of protease inhibitors and 10% NP40 was added to each fraction to yield 1 × protease inhibitors and 1% NP40. Fractions were vortexed, and aliquots (50 μl) removed for western blotting[15]. After clearing with a C7-protein A conjugate, samples were examined by immunoprecipitation/western blot[10].

Aβ ELISA

Enzyme-linked immunosorbent assay (ELISA) for $Aβ_{1\text{-total}}$ was performed as before[10]. Full-length APP and APP_S-α were not detected by either assay.

Expression and purification of IDE

Recombinant human IDE (N-terminally tagged with both polyhistidine and haemagglutinin) was expressed in BL21(DE3) *Escherichia coli* cells and purified using the TALON metal affinity kit (Clontech Laboratories), as described previously[29]. The specificity of the purified IDE was confirmed by the degradation of ^{125}I-Aβ and ^{125}I-insulin and by inhibition with cold insulin or 1,10-phenanthroline[17].

Preparation of conditioned medium for microinjection and electrophysiology

7PA2 and untransfected CHO^- cells were grown to near confluency and allowed to condition plain DMEM for ~16 h. Conditioned medium was cleared of cells (200*g* × 10 min, 4 °C) and used directly for electrophysiology or else treated to remove Aβ monomers or both Aβ monomers and oligomers. To fully deplete monomers but retain oligomers, CM (6 ml) was incubated with recombinant IDE (475 μg) for 12 h at 37 °C. In some experiments, the His-tagged IDE was then removed by metal affinity chromatography[29].

Electrophysiology

Experiments were carried out on urethane anaesthetized male adult Wistar rats. Single-pathway recordings of field excitatory postsynaptic potentials (EPSPs) were made from the stratum radiatum in the CA1 area of the hippocampus in response to stimulation of the ipsilateral Schaffer collateral/commissural pathways as described previously[16]. Test EPSPs were evoked at a frequency of 0.033 Hz and at a stimulation intensity adjusted to give an EPSP amplitude of 50% of maximum. The HFS protocol for inducing LTP consisted of 10 trains of 20 stimuli, inter-stimulus interval 5 ms (200 Hz), inter-train interval 2 s. The intensity was increased to give an EPSP of 75% of maximum amplitude during the HFS. To inject samples a cannula was implanted in the lateral cerebral ventricle (coordinates: 0.5 mm anterior to bregma and 1.0 mm right of midline) just before electrode implantation[16]. Conditioned medium samples (1.5 μl) were injected over a 2 min period, 10 min before HFS. Control injections comprised superQ water or 0.9% NaCl. LTP was measured as the mean ± s.e.m. per cent of the baseline field EPSP amplitude recorded over at least a 30-min baseline period. Similar results were obtained when the EPSP slope was measured. Statistical comparisons used paired and unpaired Student's *t*-tests.

Synthesis of γ-secretase inhibitors

The general method of ref. 30 was followed to make MWIII-20, which is carbamic acid, [3-[(L-leucyl-L-leucyl-*O*-methyl ester)carbonyl](phenylmethyl)amino]-2R-hydroxy-1S-(phenylmethyl)propyl]-1,1-dimethylethyl ester). DAPM (*N*-[*N*-3,5-difluorophenacetyl)-L-alanyl[-*S*-phenylglycine methyl ester) has been reported in patent applications

WO9822441-A2 and WO9822494-A2 filed by Athena Neurosciences and Eli Lilly. The identity of each compound was confirmed by ^{1}H-NMR and mass spectrometry.

Received 7 January; accepted 11 February 2002.

1. Selkoe, D. J. Alzheimer's disease: genes, proteins and therapies. *Physiol. Rev.* **81,** 742–761 (2001).
2. Pike, C. J. Walencewicz, A. J., Glabe, C. G. & Cotman, C. W. *In vitro* aging of β-amyloid protein causes peptide aggregation and neurotoxicity. *Brain Res.* **563,** 311–314 (1991).
3. Lorenzo, A. & Yankner, B. A. β-amyloid neurotoxicity requires fibril formation and is inhibited by congo red. *Proc. Natl Acad. Sci. USA* **91,** 12243–12247 (1994).
4. Terry, R. D. *et al.* Physical basis of cognitive alterations in Alzheimer's disease: synapse loss is the major correlate of cognitive impairment. *Ann. Neurol.* **30,** 572–580 (1991).
5. Dickson, D. W. *et al.* Correlations of synaptic and pathological markers with cognition of the elderly. *Neurobiol. Aging* **16,** 285–298 (1995).
6. Lue, L. F. *et al.* Soluble amyloid β peptide concentration as a predictor of synaptic change in Alzheimer's disease. *Am. J. Pathol.* **155,** 853–862 (1999).
7. McLean, C. A. *et al.* Soluble pool of Aβ amyloid as a determinant of severity of neurodegeneration in Alzheimer's disease. *Ann. Neurol.* **46,** 860–866 (1999).
8. Podlisny, M. B. *et al.* Aggregation of secreted amyloid β-protein into sodium dodecyl sulfate-stable oligomers in cell culture. *J. Biol. Chem.* **270,** 9564–9570 (1995).
9. Morishima-Kawashima, M. & Ihara, Y. The presence of amyloid β-protein in the detergent-insoluble membrane compartment of human neuroblastoma cells. *Biochemistry* **37,** 15247–15253 (1998).
10. Walsh, D. M., Tseng, B. P., Rydel, R. E., Podlisny, M. B. & Selkoe, D. J. Detection of intracellular oligomers of amyloid β-protein in cells derived from human brain. *Biochemistry* **39,** 10831–10839 (2000).
11. Xia, W. M. *et al.* Enhanced production and oligomerization of the 42-residue amyloid β-protein by Chinese hamster ovary cells stably expressing mutant presenilins. *J. Biol. Chem.* **272,** 7977–7982 (1997).
12. Hsia, A. Y. *et al.* Plaque-independent disruption of neural circuits in Alzheimer's disease mouse model. *Proc. Natl Acad. Sci. USA* **96,** 3228–3233 (1999).
13. Mucke, L. *et al.* High-level neuronal expression of Aβ1-42 in wild-type human amyloid protein precursor transgenic mice: synaptotoxicity without plaque formation. *J. Neurosci.* **20,** 4050–4058 (2000).
14. Hartley, D. M. *et al.* Protofibrillar intermediates of amyloid β-protein induce acute electrophysiological changes and progressive neurotoxicity in cortical neurons. *J. Neurosci.* **19,** 8876–8884 (1999).
15. Xia, W. *et al.* Presenilin complexes with the C-terminal fragments of amyloid precursor protein at the sites of amyloid β-protein generation. *Proc. Natl Acad. Sci. USA* **97,** 9299–9304 (2000).
16. Kim, J. H., Anwyl, R., Suh, Y. H., Djamgoz, M. B. & Rowan, M. J. Use-dependent effects of amyloidogenic fragments of β-amyloid precursor protein on synaptic plasticity in rat hippocampus *in vivo*. *J. Neurosci.* **21,** 1327–1333 (2001).
17. Qiu, W. Q. *et al.* Insulin-degrading enzyme regulates extracellular levels of amyloid β-protein by degradation. *J. Biol. Chem.* **273,** 32730–32738 (1998).
18. Lambert, M. P. *et al.* Diffusible, nonfibrillar ligands derived from $A\beta_{1-42}$ are potent central nervous system neurotoxins. *Proc. Natl Acad. Sci. USA* **95,** 6448–6453 (1998).
19. Walsh, D. M. *et al.* Amyloid β-protein fibrillogenesis: structure and biological activity of protofibrillar intermediates. *J. Biol. Chem.* **274,** 25945–25952 (1999).
20. Chui, D.-H. *et al.* Transgenic mice with Alzheimer presenilin 1 mutations show accelerated neurodegeneration without amyloid plaque formation. *Nature Med.* **5,** 560–564 (1999).
21. Chen, G. *et al.* A learning deficit related to age and β-amyloid plaques in a mouse model of Alzheimer's disease. *Nature* **408,** 975–979 (2000).
22. Lewis, J. *et al.* Enhanced neurofibrillary degeneration in transgenic mice expressing mutant tau and APP. *Science* **293,** 1487–1491 (2001).
23. Larson, J., Lynch, G., Games, D. & Seubert, P. Alterations in synaptic transmission and long-term potentiation in hippocampal slices for young and aged PDAPP mice. *Brain Res.* **840,** 23–35 (1999).
24. Moechars, D. *et al.* Early phenotypic changes in transgenic mice that overexpress different mutants of amyloid precursor protein in brain. *J. Biol. Chem.* **274,** 6483–6492 (1999).
25. Chapman, P. F. *et al.* Impaired synaptic plasticity and learning in aged amyloid precursor protein transgenic mice. *Nature Neurosci.* **2,** 271–276 (1999).
26. Fitzhohn, S. M. *et al.* Age-related impairment of synaptic transmission but normal long-term potentiation in transgenic mice that overexpress the human APP695SWE mutant form of amyloid precursor protein. *J. Neurosci.* **21,** 4691–4698 (2001).
27. Rochet, J. C. & Lansbury, P. T.Jr Amyloid fibrillogenesis: themes and variations. *Curr. Opin. Struct. Biol.* **10,** 60–68 (2000).
28. Chiti, F. *et al.* Designing conditions for *in vitro* formation of amyloid protofilaments and fibrils. *Proc. Natl Acad. Sci. USA* **96,** 3590–3590 (1999).
29. Chesneau, V. & Rosner, M. R. Functional human insulin-degrading enzyme can be expressed in bacteria. *Protein Expr. Purif.* **19,** 91–98 (2000).
30. Getman, D. P. *et al.* Discovery of a novel class of potent HIV-1 protease inhibitors containing the (R)-(hydroxyethyl)urea isostere. *J. Med. Chem.* **36,** 288–291 (1993).

Acknowledgements

We thank M. Rosner and V. Chesneau for the gift of the pProExH6HA IDE expression vector, B. Zheng for ELISA analysis, S. Mansourian for assistance in the preparation of illustrations and W. T. Kimberly, W. P. Esler and D. M. Hartley for discussions. Supported by NIH grants (to D.J.S. and M.S.W.) and by Enterprise Ireland and the Health Research Board Ireland (M.R. and R.A.).

Competing interests statement

The authors declare that they have no competing financial interests.

Correspondence and requests for materials should be addressed to D.J.S. (e-mail: dselkoe@rics.bwh.harvard.edu).

A global disorder of imprinting in the human female germ line

Hannah Judson, Bruce E. Hayward, Eamonn Sheridan & David T. Bonthron

University of Leeds, Molecular Medicine Unit, St. James's University Hospital, Leeds LS9 7TF, UK

Imprinted genes are expressed differently depending on whether they are carried by a chromosome of maternal or paternal origin. Correct imprinting is established by germline-specific modifications; failure of this process underlies several inherited human syndromes[1–5]. All these imprinting control defects are *cis*-acting, disrupting establishment or maintenance of allele-specific epigenetic modifications across one contiguous segment of the genome. In contrast, we report here an inherited global imprinting defect. This recessive maternal-effect mutation disrupts the specification of imprints at multiple, non-contiguous loci, with the result that genes normally carrying a maternal methylation imprint assume a paternal epigenetic pattern on the maternal allele. The resulting conception is phenotypically indistinguishable from an androgenetic complete hydatidiform mole[6], in which abnormal extra-embryonic tissue proliferates while development of the embryo is absent or nearly so. This disorder offers a genetic route to the identification of *trans*-acting oocyte factors that mediate maternal imprint establishment.

Although normally sporadic, complete hydatidiform mole (CHM) is occasionally familial, with affected women repeatedly having pregnancies of this type. These repetitive CHMs are not androgenetic but biparental (BiCHM)[7–9]. By analogy to disorders like Prader–Willi syndrome (which can result from sporadic uniparental disomy or from familial imprinting control mutations), we considered that BiCHM might arise from a global inherited failure of maternal imprinting.

We studied the sixth molar pregnancy of the index case in a BiCHM family with complex consanguinity, originating from the Mirpur region of Pakistan. We demonstrated biparental origin of the BiCHM DNA using markers on six autosomes.

Imprinted genes are associated with differentially methylated regions (DMRs), either 'primary' (established during gametogenesis) or 'secondary' (established later in embryogenesis). We used bisulphite sequencing[10] to compare methylation in the BiCHM and suitable controls, including uniparental DNAs and first-trimester chorionic villus samples, which like CHMs, are of trophoblastic origin.

The Beckwith–Wiedemann region of 11p15 contains two putative primary imprint control regions, at *H19* and *KCNQ1OT1*, ~500 kilobases (500 kb) apart. The DMR ~2-kb upstream of *H19* normally shows paternal-specific germline methylation[11], and is therefore an important control locus (Fig. 1a). Parthenogenetic (Pg) and androgenetic (Ag) control DNAs were respectively completely unmethylated and completely methylated at all CpG dinucleotides, as expected. The BiCHM DNA shows a differentially methylated pattern, like that of normal controls. Cloned polymerase chain reaction (PCR) products from BiCHM were either almost completely methylated or completely unmethylated, as expected for paternal or maternal alleles, respectively.) This maintenance of normal *H19* differential methylation in the BiCHM is as predicted, if only imprinting in the female germ line is affected.

At loci with a maternal methylation imprint (Fig. 1b–e), a very different pattern is seen. The *KCNQ1OT1* primary DMR[12,13] becomes methylated during oogenesis[14]. As expected, our normal control DNAs are uniformly haplo-methylated (C and T bands of similar intensity at each original CpG position), and the partheno-